Catal Lett (2017) 147:2332–2339
DOI 10.1007/s10562-017-2112-7

Catalytic Activity of Crystallographically Characterized Organic–Inorganic Hybrid Containing 1,5-Di-amino-pentane Tetrachloro Manganate with Perovskite Type Structure

Paramita Mondal[1,4] · Seham Kamal Abdel-Aal[2,3] · Debasis Das[4] · Sk Manirul Islam[1]

Received: 27 March 2017 / Accepted: 9 June 2017 / Published online: 5 July 2017

Abstract Layered 2D organic–inorganic hybrid perovskite (OIHS) of the diammonium series, 1,5 di-aminepentane tetrachloro mangenate ($[NH_3–(CH_2)_5–NH_3]$ $MnCl_4$) was prepared by slow evaporation and reducing temperature method and characterized by single crystal X-ray diffraction analysis. Its structure consists of organic cation, $[NH_3(CH_2)_5NH_3]^{+2}$ extended in a zigzag fashion and inorganic anion, $[MnCl_6]^{-2}$ where Mn^{2+} is coordinated by six Cl^- ion in octahedral fashion. The organic and inorganic segments are alternately stacked along *c*-axis where inorganic layer is extended through corner-shared octahedra sandwiched by the di-aminopentane molecules. The layers (organic and inorganic) were connected to each other through N–H···Cl hydrogen bonds and van-der Waals interaction to build cation–anion–cation cohesion. The hybrid crystal had orthorhombic non-centrosymetric system having $I2_12_12_1$ space group with unit cell parameters a = 7.1742(3) Å, b = 7.3817(3) Å, c = 23.9650(10) Å, V = 1269.13 Å^3 and Z = 4. The hybrid exhibited excellent catalytic activity towards sulphide and alkene oxidation using aqueous H_2O_2 as an oxidant.

Graphical Abstract OIHS of the diammonium series $[NH_3–(CH_2)_5–NH_3]$ $MnCl_4$; 1,5 di-aminepentane tetrachloro mangenate were prepared by slow evaporation and temperature decrease method, characterized by single crystal X-ray diffraction. This complex exhibits excellent catalytic activity towards sulphide oxidation and alkene oxidation using aqueous H_2O_2 as an oxidant.

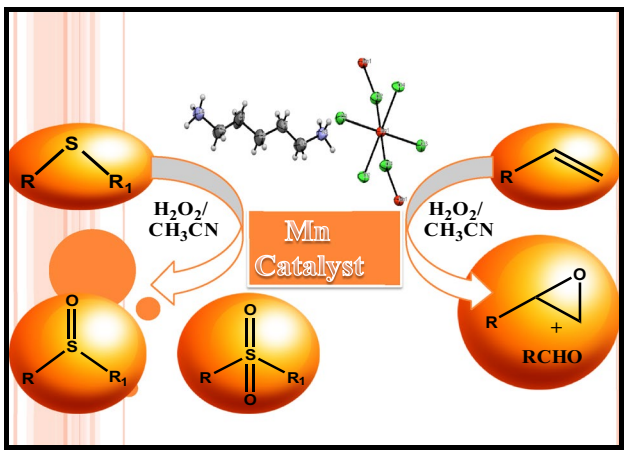

Keywords Layered 2D organic–inorganic hybrid · Perovskite type Mn complex · Alkene oxidation · Sulfide oxidation · Hydrogen peroxide

1 Introduction

Nowadays significant attention has been devoted to the preparation and characterization of organic–inorganic

✉ Seham Kamal Abdel-Aal
seham@sci.cu.edu.eg

✉ Debasis Das
ddas100in@yahoo.com

✉ Sk Manirul Islam
manir65@rediffmail.com

[1] Department of Chemistry, University of Kalyani, Nadia, Kalyani 741235, India

[2] Department of Physics, University of Cairo, Giza 12613, Egypt

[3] Egypt Nanotechnology center EGNC, Sheik Zayied city, Egypt

[4] Department of Chemistry, The University of Burdwan, Burdwan, West Bengal 713104, India

multi-layered perovskites hybrids (OIHs) to tailor their structural features and tuning their physical as well as chemical properties. The general formula of diammonium halide perovskite hybrids are A2MX4, where A is an organic cation, M, a divalent cation while X is a halogen. The perovskite type OIHs of diammonium series having formula $[NH_3–(CH_2)n–NH_3]MX4$ (where n = 2, 3, 4… etc. and M = Mn, Cu, Pb, Fe, Co; X = Cl, Br, I) had extensively been investigated for their interesting physical and chemical properties, reduced dimension and presence of numerous structural phase transitions [1–10]. The structures and properties of OIHs depend on the characteristics of the organic cation $[NH_3–(CH_2)n–NH_3]^{++}$ (alkyl chain length and attached functionalities), the inorganic anion $MX_4^{-\ -}$ (coordination geometry of the cation) and nature of halide [3–10]. Studies in this area lead to innovation of advanced materials, solar cells, smart microelectronic, micro-optical, photonic components and self-assembled quantum well applications [5, 6, 8]. The simplest 2D layered hybrids consist of $MX^{-2}{}_6$ corner-sharing metal halide octahedra separated by mono-layers of the organic moiety. The cavities between the octahedron were occupied by the terminal NH_3 of the organic moieties, $[NH_3–(CH_2)n–NH_3]$ via formation of N–H···Cl hydrogen bonds with the halide of the octahedron.

Selective oxidation of organic sulfides to sulfoxides is one of the key reactions in the domain of organo oxidation chemistry because of the prospective use of sulfoxides as synthetic intermediates for the creation of many chemically and biologically active molecules [11, 12]. The prime synthetic path for the preparation of these expensive materials is via oxidation of the corresponding sulfides. Several reagents used for this key transformation includes stoichiometric or catalytic amounts of both organic and inorganic reagents [13–15]. The exploitation of 'green oxidants' such as molecular oxygen and hydrogen peroxide are attractive, since they are readily available, inexpensive, and environment friendly, with a formation of water as sole by-product [16]. Oxidation of sulfides with H_2O_2 is slow; hence extensive studies have been performed to develop new catalysts for this reaction [16–19]. Disadvantages of this sulfoxidation reaction include difficulties to arrest the oxidation at the sulfoxide stage, and formation of toxic waste. Hence, there is a need to develop new catalysts to overcome these drawbacks.

Alkene oxidation is one of the basic reactions in industrial organic synthesis because aldehydes and ketones are key intermediates for the manufacture of wide variety of valuable products [20, 21]. Aldehydes and ketones find a range of applications in the industry of perfumery, pharmaceutical, dyestuff and agrochemicals [22–24]. So, alkene oxidation under mild conditions is challenging while transition metal catalyzed the oxidation of the former is a promising approach. However, the development and implementation of catalytic processes to eliminate the use of hazardous reactants and reduce waste generation is an important goal. In this context, use of H_2O_2 as green oxidant is an alternative approach.

Herein, we report the synthesis, X-ray single crystal structure, sulphide and alkene oxidation activities of a new layered 2D OIHs of the diammonium series, $(NH_3–(CH_2)_5–NH_3]\ MnCl_4)$. To the best of our knowledge, alkene and sulphide oxidation using aqueous H_2O_2 in presence of catalytic amount of Mn-hybrid (C5MnCl) has been performed for the first time.

2 Experimental

2.1 Preparation of $[NH_3–(CH_2)_5–NH_3]\ MnCl_4$

Perovskite hybrid of $[NH_3–(CH_2)_5–NH_3]\ MnCl_4$ was prepared by reacting ethanol solution of both $[NH_3–(CH_2)_5–NH_3]\ Cl_2$ and $MnCl_4.4H_2O$ (1:1 mol ratio) at 70° C for 1 h followed by gradual cooling to room temperature. Thereby, pink crystals precipitated out. Chemical analysis and single crystal X-ray diffraction analysis indicated its chemical formula as $[NH_3–(CH_2)_5–NH_3]\ MnCl_4$ (henceforth **C5MnCl**).

2.2 Characterization

2.2.1 Single Crystal X-ray Diffraction Analysis

The single crystal X-ray crystallographic data were collected on Enraf–Nonius 590 Kappa CCD single crystal diffractometer with graphite monochromator using MoKα (λ = 0.71073 Å). The intensities were collected at room temperature (298 K) using φ–ω scan mode; the crystal to detector distance was 40 mm. The cell refinement and data reduction were carried out using Denzo and Scalepak programs [25] The crystal structure was solved by the direct method using SIR92 program [26] which revealed the positions of all non-hydrogen atoms and refined by the full matrix least square refinement based on F2 using maXus package [27]. Short average multi-scanning absorption corrections were applied to all data using SORTAV program [28]. The temperature factors of all non-hydrogen atoms were refined anisotropically, then hydrogen atoms were introduced as a riding model with C–H = 0.96 Å and refined isotropically. Molecular graphics were prepared using ORTEP and Mercury softwares [29].

3 Results and Discussion

3.1 Description of the Structure of C5MnCl

The structure of **C5MnCl** consists of organic dication $[NH_3–(CH_2)_5–NH_3]^{+2}$ extended in a zigzag structure and inorganic dianion $MnCl_4^{2-}$ coordinated by six Cl atoms in octahedral topology, $[MnCl_6]^{2-}$. The organic and inorganic structures were alternatively stacked along *c* axis, where inorganic layers were extended corner-shared octahedra sandwiched by the di-aminopentane molecules. The layers (organic and inorganic) were connected with each other through N–H···Cl hydrogen bonds and van-Der Waals interaction as to build cation–anion–cation cohesion. The hybrid crystallized in orthorhombic space group $I2_12_12_1$, having unit cell parameters: a = 7.1742(3) Å, b = 7.3817(3) Å, c = 23.9650(10) Å, V = 1269.13 Å^3 and Z = 4. The structure was solved by using 2760 independent reflections down to R value of 0.053. While Table 1 shows the crystallographic parameters of **C5MnCl**, Fig. 1 presents its molecular structure. Figure 2 show the unit cell along 010 plane.

3.2 UV–Vis and FTIR Spectra Analysis

It is clearly noted from Fig. 1a that the ligand did not coordinate to manganese center. Rather, the ligand is protonated and this protonated cation interacted with the manganese containing anion. So, that is also reflected from the UV–Vis spectrum of the complex. The absorption spectrum (Fig. 3) of ethanol solution of **C5MnCl** show peaks at ~209 nm and 259.0 nm which may be attributed to the intra-ligand (n–π* and π–π*) charge transfer processes. Moreover, a very weak absorption at 520 nm, characteristics of Mn(II) center was also observed.

Figure 4 show the FTIR spectrum of **C5MnCl** in the range 4000–400 cm^{-1}. The bands at region 4000–3000 cm^{-1} were due to internal stretching of the diammonium cation. The C–H bonds of the protonated ligand show IR bands in the range 3188−3060 cm^{-1}. Moreover, N–H stretching bands were observed in the range 3360−3100 cm^{-1}. The unique band at 2941−2885 cm^{-1} were characteristics and indication of hydrogen bond formed [1, 4, 30].

The band at 1492 cm^{-1} was probably due to the (NH_3) symmetric deformation mode. The strong band at 1583 cm^{-1} was assigned to asymmetric mode, δ_{as} (NH_3). Bands near 1200 cm^{-1} were assigned to the wagging mode of the CH_2 group. The coupling with the $(NH_3)^+$might be the reason for strong enhancement of the intensity of CH_2 stretching frequency. For **C5MnCl**4, δ_r (CH_2) was found at 1400–1123 cm^{-1}, and wagging coupled with $(NH_3)^+$was found at 1176 cm^{-1}. Bands at

Table 1 Single crystal X-ray diffraction parameters of **C5MnCl**

	C5MnCl
Empirical formula	$C_5H_{16}N_2MnCl_4$
M_r	300.94
Space group	Orthorhombic $I2_12_12_1$
A	7.1742 (3) Å
B	7.3817 (3) Å
C	23.9650 (10) Å
β	90°
V	1269.13 (9) Å^3
Z	4
D_x	1.575 Mg m^{-3}
Radiation type	Mo *K*α
λ	0.71073 Å
θ_{max}	34.97°
μ	1.84 mm^{-1}
T	298 K
Shape	Cube
Color	Pink
Measured reflection	7557
Independent reflections	2760
Observed reflections	1482
Criterion	I > 2.00 sigma(I)
R_{int}	0.055
H	−10 →11
K	−11→11
L	−32 →38
R (all)	0.122
R (gt)	0.053
wR (ref)	0.171
wR (gt)	0.134
S (ref)	0.895
Δ/σ_{max}	0.416
$\Delta\rho_{max}$	0.524 eÅ^{-3}
$\Delta\rho_{min}$	−0.665 eÅ^{-3}
Reference	This work

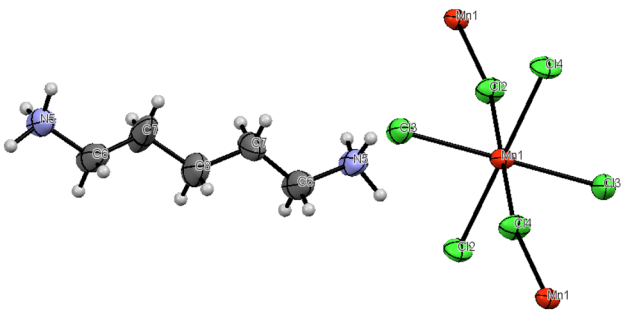

Fig. 1 Molecular structure of hybrid **C5MnCl**

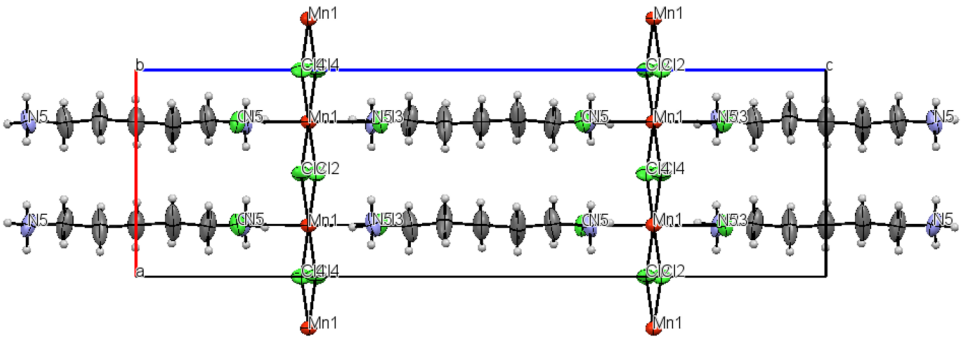

Fig. 2 Layer structure of **C5MnCl** in the unit cell along 010 plane

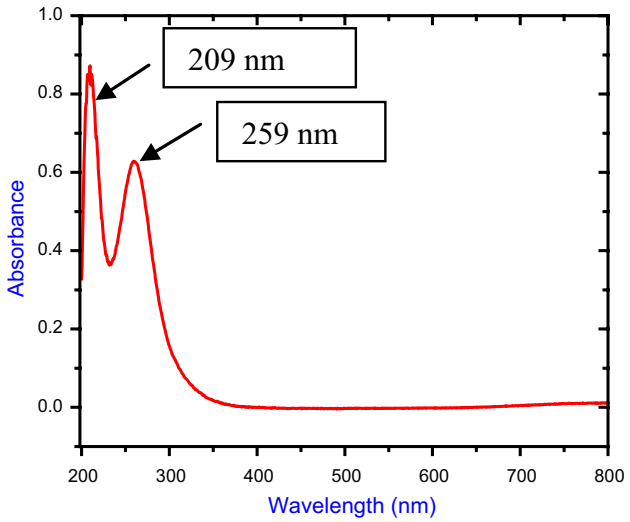

Fig. 3 UV–vis spectrum of **C5MnCl**

900–700 cm^{-1} were assigned to the CH_2 rocking mode δ_r (CH_2). Bands below 700 cm^{-1} were assigned to the stretching mode of C–N bond. The observed IR bands were in good agreement to the similar compounds found in literature [1, 4].

3.3 General Procedure for Oxidation Reactions

The solution phase oxidation reactions were carried out in a double necked round bottom flask equipped with a water condenser and refluxed at different temperatures under vigorous stirring for a certain period of time over an oil bath. Substrates (5 mmol) were dissolved in acetonitrile (5 mL) along with 5 mg **C5MnCl** and 10 mmol of H_2O_2 (30% aqueous solution). Monitoring of product formation was performed using Varian 3400 gas chromatographic instrument equipped with a 30 m CP-SIL8CB capillary column and a FID detector. All products were identified by GC by comparing with the reference samples.

3.4 Catalytic Activity

*3.4.1 Oxidation of Sulfides with H_2O_2 Using **C5MnCl** Catalyst*

For optimization of the reaction conditions, oxidation of diphenyl sulfide was carried out as a probe reaction (Scheme 1). The **C5MnCl** catalyst was very efficient for the oxidation of diphenylsulfide to produce sulfoxide as a major product. First, the oxidation of diphenylsulfide with H_2O_2 using **C5MnCl** catalyst was examined in several polar and non-polar solvents (Table 2). Quantitative yields were obtained with polar solvents like acetonitrile, dimethylformamide and methanol (Table 2, runs 1–3), however, the efficiency of the catalyst was not satisfactory in non-polar solvents like toluene and *p*-xylene (Table 2, runs 5, 6). The higher catalytic activity in acetonitrile was attributed to its dielectric constant, polarity and higher miscibility of the organic substrate and H_2O_2. It was observed that less polar solvents constituted a heterogeneous system with aqueous hydrogen peroxide which was ineffective. The reaction temperature played a significant role on the catalytic activity as evident from Fig. 5. At room temperature, moderate yield of the product was observed. Upon increase of reaction temperature to 40 °C, complete conversion of diphenylsulfide, along with the highest selectivity to yield the corresponding sulfoxide were observed. At much higher temperature (60 °C), conversion efficiency remain unaltered however the selectivity of product yield decreased. The catalytic activity of **C5MnCl** for oxidation of diphenylsulfide was also investigated using a variable amount of H_2O_2 (n = 3). Table 2 indicated that the conversion to the product increased with increasing amount of H_2O_2 (from 5 mmol, run 7 to 10 mmol, run 1). However, further increase of H_2O_2 to 15 mmol caused no significant increase in the conversion efficiency (Table 2, run 8) under said reaction conditions. Rather, the selectivity of yielding sulfoxide decreased at 15 mmol H_2O_2. This might be due to further oxidation of sulfoxide to corresponding sulfone derivative. The results were presented in Fig. 6. With the increase of the catalyst

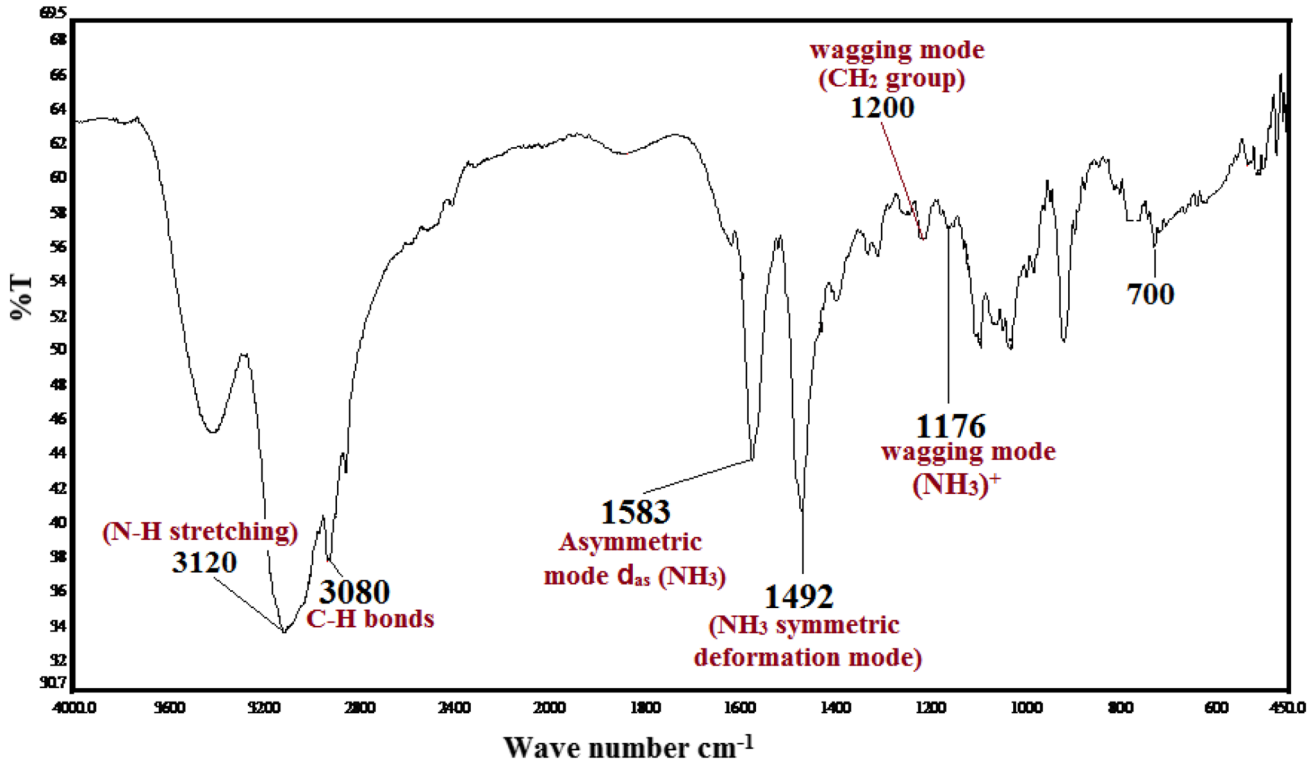

Fig. 4 FTIR spectrum of **C5MnCl**

Scheme 1 Oxidation of diphenyl sulfide

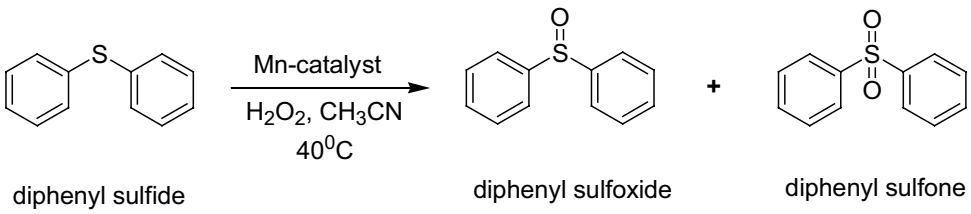

Table 2 Effect of different reaction parameters on the oxidation of diphenyl sulfide using **C5MnCl** catalyst

Run	Solvent	Amount of 30% aq. H_2O_2 (mmol)	Conversion (%)[a]
1	CH_3CN	10	97
2	DMF	10	56
3	Methanol	10	38
4	$CHCl_3$	10	20
5	Toluene	10	12
6[b]	*p*-Xylene	10	07
7	CH_3CN	5	36
8	CH_3CN	15	87
9	CH_3CN	–	No reaction

Conditions: Diphenyl sulfide (5 mmol), solvent (5 mL); catalyst (5 mg), temp. (40 °C), time 5 h

[a]Conversion and selectivity were determined by GC

[b]Products were characterized by GC by comparing with the authentic samples

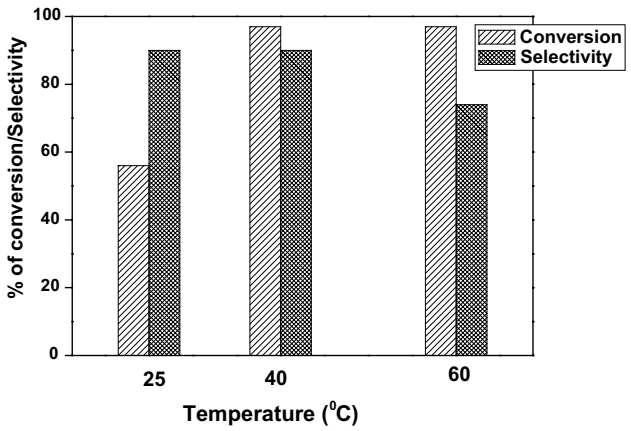

Fig. 5 Effect of temperature on the oxidation of diphenyl sulfide using **C5MnCl** catalyst. Reaction conditions: diphenyl sulfide (5 mmol), CH_3CN (5 mL); **C5MnCl** catalyst (5 mg), Time, 5 h

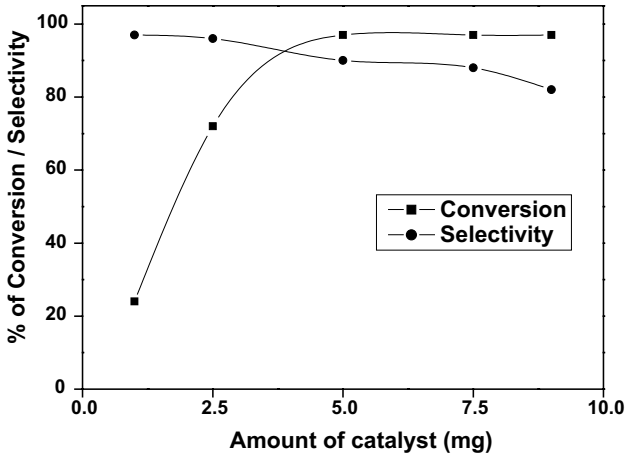

Fig. 6 Effect of catalyst load on the oxidation of diphenyl sulfide. Reaction conditions: diphenyl sulfide (5 mmol), CH_3CN (5 mL); temperature (40 °C), time, 5 h

load to 2.5 mg, the conversion efficiency increased to 72% while a little amount of sulfone was detected. A further increase of catalyst load to 5 mg increased the conversion to 97%. Interestingly, at a much higher amount of the catalyst (7.5 and 9 mg), the conversion efficiency remained almost constant, however, the selectivity of sulfoxide production was reduced. These findings indicated that the oxidation of sulfide was highly dependent on the amount of the catalyst. A blank experiment in presence of oxidant under same experimental conditions without **C5MnCl** was also investigated and found a very poor conversion of diphenylsulfide. Thus, it was concluded that 5 mg of **C5MnCl** catalyst, 10 mmol 30% H_2O_2 in acetonitrile medium was the optimum condition for the oxidation of sulfides to sulfoxides with very good selectivity. Moreover, in absence of H_2O_2, **C5MnCl** catalyst alone failed to oxidize sulfides (Table 2, run 9).

For wider application of the catalyst, oxidation of other sulfides were also examined (Table 3). Substrate scope was extended to various aliphatic and aromatic sulfides. In all cases, sulfoxides were selectively obtained under optimum reaction conditions. A series of substrates, aryl alkyl, aryl allyl and dialkylsulfides, could be oxidized to the corresponding sulfoxides in good yields. The reactivity and conversion efficiencies were dependent on the nature of the substituent present in the ArSMe. The introduction of electron donating substituents in the phenyl ring of ArSMe accelerated the rate whereas the electron withdrawing substituents retarded the rate (Table 3, runs 7 and 8). The sulfur center of substituted sulfides containing other oxidation prone functional groups such as C–C and OH (Table 3, runs 9 and 10) gave good conversion with the present catalyst.

3.4.2 Oxidation of Alkenes with H_2O_2 Using C5MnCl Catalyst

The excellent catalytic activity of **C5MnCl** for sulfide oxidation motivated us to explore its potentiality for alkene oxidation. For optimization of reaction conditions, oxidation of styrene was monitored as a probe reaction using **C5MnCl** as catalyst and H_2O_2 as an oxidant while benzaldehyde was formed as the major product (Scheme 2). The results of the control experiment revealed (Table 4) that the presence of both catalyst and oxidant were essential for the oxidation reaction to occur (run11). In absence of **C5MnCl** catalyst, the oxidation proceeded only up to 8% after 24 h (run 12).

In search of suitable reaction conditions for maximum oxidation of styrene, the effect of solvent, concentration of oxidant (moles of H_2O_2 per moles of styrene), and reaction temperature were studied. At first, oxidation of styrene was studied in different solvents like methanol, acetone, DMF and CH_3CN (Table 4, runs 1–4). As highest conversion

Table 3 Oxidation of sulfides using 30% H_2O_2 catalyzed by Mn-catalyst

Entry	Substrates	Conversion (%)/time (h)[a]	Product selectivity (%) sulfoxide/sulfone[a,b]	TON	TOF h^{-1}
1	$PhSCH_3$	99/3	92/8	298	99
2	$PhSC_2H_5$	95/4	89/11	286	71
3	PhSPh	97/4	90/10	292	73
4	$PhSCH_2Ph$	88/5	87/13	265	53
5	p-$CH_3C_6H_4SCH_3$	83/6	85/15	250	42
6	p-$NO_2C_6H_4SCH_3$	98/4	88/12	295	74
7	$C_4H_9SC_4H_9$	89/4	87/13	268	67
8	$PhSCH_2CH{=}CH_2$	71/6	80/20	213	36
9	$PhSC_2H_4OH$	84/6	83/17	253	42

Conditions: Sulfide (5 mmol); 30% aq H_2O_2 (10 mmol); CH_3CN (5 ml); catalyst (5 mg) temperature 40 °C

[a]Conversion and selectivity were determined by GC

[b]Products were characterized by GC by comparing with the authentic samples

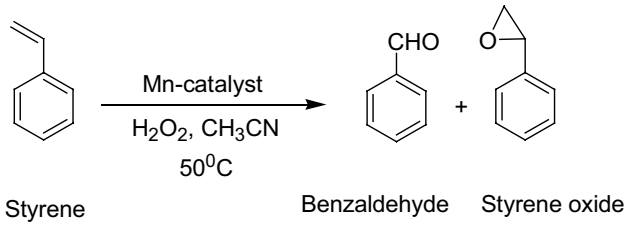

Scheme 2 Oxidation products of styrene

Table 4 The effect of different reaction parameters on the oxidation of styrene using **C5MnCl** catalyst

Run	Solvent	Temperature (°C)	H_2O_2 to substrate mole ratio	Conversion (%)[a]
1	Methanol	50	2:1	38
2	Acetone	50	2:1	47
3	DMF	50	2:1	78
4	CH_3CN	50	2:1	93
5	CH_3CN	50	0.5:1	29
6	CH_3CN	50	1:1	72
7	CH_3CN	50	3:1	91
8	CH_3CN	30	2:1	18
9	CH_3CN	40	2:1	58
10	CH_3CN	60	2:1	93
11	CH_3CN	50	0:1	No reaction
12[b]	CH_3CN	50	2:1	8

Conditions: styrene (5 mmol), solvent (5 mL); catalyst (5 mg), time (6 h)

[a]Conversion was determined by GC

[b]In absence of catalyst

was found in acetonitrile medium, it was chosen as the reaction medium. The effect of concentration of H_2O_2 on the oxidation of styrene was illustrated in Table 4. Different H_2O_2/styrene molar ratios (0.5:1, 1:1, 2:1 and 3:1) were employed while keeping fixed amount of styrene (1.0 mmol) and catalyst (5 mg) in CH_3CN (5 mL) medium at 50 °C. Increasing H_2O_2/styrene ratio from 0.5:1 to 2:1 increased the conversion efficiency from 29 to 93%. The Further increase had resulted in reduced the conversion. The maximum styrene conversion was found in the case of 2:1 mol ratio. The performance of the catalyst was studied at four different temperatures, viz. 30 (room temperature), 40, 50 and 60 °C, keeping fixed amount of styrene (5 mmol), H_2O_2 (10 mmol) and catalyst (5 mg) in 5 mL CH_3CN (Table 4, runs 4, 8–10). A maximum of 93% conversion was achieved by carrying out the reaction at 50 °C. At lower temperature, the conversion efficiency was low. At 60 °C, the initial conversion of styrene was high than at 50 °C but the selectivity of oxidation lost to an extent. Therefore, 50 °C was chosen as the optimum temperature for all catalytic oxidation reactions of olefins.

These optimized reaction conditions were applied to the oxidation reactions of other olefins by **C5MnCl** catalyst and the results were shown in Table 5. This catalyst efficiently converted olefins to the corresponding allylic products in presence of H_2O_2. In the oxidation of cyclohexene, allylic products, 2-cyclohexene-1-one and 2-cyclohexene-1-ol were obtained. Substituted styrene selectively produced corresponding aldehydes. Acetophenone was detected in the oxidation of α-methyl styrene as a major product. *Trans*-stilbene was also oxidized by this catalyst in high yields and gave benzaldehyde as a major product

Table 5 Oxidation of alkenes by **C5MnCl** catalyst in presence of 30% H_2O_2

Run	Substrates	Conversion (%)[a]/ time (h)	Product selectivity (%)[b]	TON	TOF h^{-1}
1	Cyclohexene	83/6	2-Cyclohexene-1-one (67) 2-Cyclohexene-1-ol (30)	250	42
2	Styrene	93/6	Benzaldehyde (88) Styrene oxide (12)	280	47
3	4-Methylstyrene	74/6	4-Methyl benzaldehyde (81) 4-Methylstyrene epoxide (17)	223	37
4	4-Chlorostyrene	72/6	4-Chloro benzaldehyde (77) 4-Chlorostyrene epoxide (23)	217	36
5	4-Nitrostyrene	85/6	4-Nitro benzaldehyde (80) 4-Nitro styrene oxide (20)	256	43
6	α-Methyl styrene	84/6	Acetophenone (100)	253	41
7	*Trans*-Stilbene	70/8	Benzaldehyde (75) Benzil (18)	211	26
8	α-Pinene	56/8	Verbenol(23) Verbenone (56) α-Pinene oxide (21)	169	21

Conditions: styrene (5 mmol), solvent (5 mL); catalyst (5 mg), time (6 h)

[a]Conversion was determined by GC

[b]In absence of catalyst

along with small amount of benzil. This catalyst shows good activity for oxidation of α -pinene, where major products found were verbenone and verbenol. We have also compared the catalytic results for oxidation of alkenes with other reported catalyst in the literature [31, 32]. Our catalyst shows comparable results with other reported catalysts [31, 32].

4 Conclusion

We have reported the synthesis and single crystal X-ray structure of 2D hybrid perovskite of $[[NH_3–(CH_2)_5–NH_3]\ MnCl_4$ (cadverin salt). The hybrid crystallizes as an orthorhombic system having space group $I2_12_12_1$ non-centrosymmetric, with unit cell parameters a = 7.1742 (3) Å, b = 7.3817 (3) Å, c = 23.9650 (10)Å and Z (the number of molecules per unit cell) = 4. This hybrid perovskite show excellent catalytic activity for oxidation of sulphide and alkene using H_2O_2 as an oxidant, observed for the first time in the area of organic–inorganic hybrids.

5 Supplementary materials

All crystallographic data for the structure reported in this manuscript may be obtained free of charge through Cambridge Crystallographic Data Centre as supplementary publication, deposit number. CCDC. 1401387. Copies of the data may be obtained on application to CCDC, 12 Union Road, Cambridge CB2 1EZ, UK (fax: +44 1223 336 033; e-mail: deposit@ccdc.cam.ac.uk).

Acknowledgements P.M. is thankful to the University Grant Commission (UGC) for funding in the form of Dr. D.S. Kothari post-doctoral research fellowship (Award no. F4-2/2006 (BSR)/CH/15–16/023). We sincerely thank Department of Chemistry of the University of Burdwan for infrastructural facilities. S.M.I. acknowledges the Council of Scientific and Industrial research, (CSIR, project reference no. 02(0284)/16/EMR-II), New Delhi, Govt. India, and Department of Science and Technology, Govt. of West Bengal (DST-W.B.), Project Reference Number 811(Sanc.) /ST/P/S&T/4G-8/2014, dated: 04/01/2016, for funding. We acknowledge Department of Science and Technology (DST) and University Grant Commission (UGC) New Delhi, India for providing support to the Department of Chemistry, University of Kalyani under PURSE, FIST and SAP program. S. K. A. is grateful to the financial support of Faculty of Science, Cairo University, Egypt.

References

1. Abdel-Aal SK, Abdel-Rahman AS (2017) J Cryst Growth 457:282
2. Mostafa MF, Abdel-Aal SK, Tammam AK (2014) Ind J Phys 88(1):49
3. Mostafa MF, El-khiyami SS, Abdel-Aal SK (2017) J Mol Struct 1127:59
4. Abdel-Aal SK (2017) Solid State Ionics 303:29
5. Pradeesh K, Baumberg JJ, Vijaya Prakash G (2009) Appl Phys Lett 95(3):033309
6. Pradeesh K, Yadav GS, Singh M, Vijaya Prakash G (2010) Mater Chem Phys 124(1):44
7. Wei Y, Audebert P, Galmiche L, Lauret JS, Deleporte E, (2014) Materials 7(6):4789
8. Mitzi DB (2001) Dalton Trans 1:1
9. González-Carrero S, Galian RE, Pérez-Prieto J, (2015) Part Syst Charact 32(7):709
10. Maris T, Bravic G, Chanh NB, Leger JM, Bissey JC, Villesuzanne A, Zouari R, Daoud A, (1996) J Phys Chem Solids 57(12):1963.
11. Drabowicz J, Kielbsinski P, Mikolajczyk M, Patai S, Rappoport Z, Stirling C (eds) (1988) The chemistry of sulphone and sulphoxide. Wiley, New York
12. Frenanez I, Khiar N (2003) Chem Rev 103:3651
13. Romanelli GP, Vázquez PG, Tundo P (2005) Synlett 1:75
14. Kaczorowska K, Kolarska Z, Mitka K, Kowalski P (2005) Tetrahedron 61:8315
15. Bahrami K (2006) Tetrahedron Lett 47:2009
16. Lane BS, Burgess K (2003) Chem Rev 103:2457
17. Venkat-Reddy C, Verkade JG (2007) J Mol Catal A 272:233
18. Jeyakumar K, Chand DK (2006) Tetrahedron Lett 47:4573
19. Kirihara M, Yamamoto J, Noguchi T, Hirai Y (2009) Tetrahedron Lett 50:1180
20. Choudary BM, Bharathi B, Reddy CV, Kantam ML, (2002) J Chem Soc Perkin Trans 1:2069
21. Shaabani A, Rezayan AH (2007) Catal Commun 8:1112
22. Fredrich B, Gerhartz W (eds.) (1985) Ullmann's encyclopedia of industrial chemistry, vol 3 Wiley, Weinheim, New York, p. 470
23. Kroschwitz JI, Othmer K (1992) Encyclopedia of chemical technology. Wiley, New York
24. Ullmann F (2003) Ullmanns encyclopedia of industrial chemistry. Wiley, Weinheim
25. Otwinowski Z, Minor W, Carter CW, Jr., Sweet RM (ed) (1997) Cell refinement: HKL scalepack. in: Methods in enzymology, vol 276 Publishing Academic Press, New York, p 30
26. Altomare A, Cascarano G, Giacovazzo C, Guagliardi A, Burla MC, Polidori G, Camalli M, (1994) J Appl Cryst 27:435.
27. Mackay S, Gilmore CJ, Edwards C, Stewart N, Shankland K, maXus Computer Program for the Solution and Refinement of crystal Structures. Bruker Nonius, The Netherlands, MacScience, Japan and The University of Glasgow (1999).
28. Blessing RH, (1995) Acta Cryst A 51:33.
29. Johnson CK, ORTEP–II (1976) A fortran thermal-ellipsoid plot program, Report ORNL-5138, Oak Ridge National Laboratory, Oak Ridge, Tennessee. USA
30. Dhara K, Sarkar K, Srimani D, Saha SK, Chattopadhay P, Bhaumik A (2010) Dalton Trans 39:6395
31. Nandi M, Roy P, Uyama H, Bhaumik A (2011) Dalton Trans 40:12510
32. Paul L Banerjee B, Bhaumik A, Ali M, (2016) J Solid State Chem 237:105